J Nanopart Res (2018) 20: 219
https://doi.org/10.1007/s11051-018-4325-0

RESEARCH PAPER

# Green preparation of Pd nanoparticles on SBA-15 via supercritical fluid deposition and application on Suzuki–Miyaura cross-coupling reaction

**Fatma Ulusal · Ebru Erünal · Bilgehan Güzel**

Received: 5 April 2018 / Accepted: 9 August 2018 / Published online: 17 August 2018


**Abstract** A well-dispersed green Pd/SBA-15 catalyst with an average size of 13.7 nm and 492.6 $m^2/g$ BET surface area is prepared via supercritical fluid deposition method with a new bipyridyl precursor that enables reduction at mild conditions at 80 °C and 17.2 MPa. The catalytic performance of Pd/SBA-15 prepared using $scCO_2$ with hydrogen reduction was assessed for Suzuki–Miyaura coupling reaction of bromobenzene and phenylboronic acid that was chosen as a model coupling reaction. The catalyst was tested in six different solutions and in three organic and inorganic bases during reactions. In general, the effect of bases is investigated when solvents are held constant and $K_2CO_3$ appears to have the best results in the activity studies used. For each of the 3 bases used, the highest catalytic activity was reached as the result of the solvent system being ethanol/water (1:1). The highest catalytic conversion was obtained in the ethanol-$K_2CO_3$ solvent-base pair. The catalyst synthesized in this study exhibited high activities and TON value was found as 160.8 at room temperature.

F. Ulusal · B. Güzel
Chemistry Department, The Faculty of Arts and Sciences, Çukurova University, 01330 Adana, Turkey

F. Ulusal (✉)
Clinical Biochemistry Department, The Faculty of Medicine, Gaziantep University, 27310 Gaziantep, Turkey
e-mail: fatma_ulusal@hotmail.com

E. Erünal
Chemical Engineering Department, The Faculty of Ceyhan Engineering, Çukurova University, 01950 Adana, Turkey

**Keywords** SBA-15 · Suzuki–Miyaura cross-coupling reaction · Supercritical deposition · Green chemistry · Palladium nanoparticle

## Introduction

Green methods are more preferred in industrially important reactions due to the environmental concerns and thanks to developments in green chemistry. Especially in organic synthesis, alternative green processes can be eco-friendly and reduce costs (Beckman 2004). In this sense, the use of supercritical solvents instead of conventional organic solvents is an effective approach. The most commonly used green solvents for alternative in organic synthesis are supercritical carbon dioxide, supercritical, and subcritical water (Gang et al. 2003; Ulusal et al. 2015). Supercritical carbon dioxide ($scCO_2$) offers real potential as an alternative, environmentally benign reaction medium for the green preparation of organic molecules because it is nontoxic, cheap, and easily separable from reaction media (Meng et al. 2018; Hiramatsu and Hori 2010). Thanks to these features, it gains importance day by day and is used as an alternative solvent. Especially, supercritical fluids have been used in various techniques such as organic synthesis (Ulusal et al. 2015; Morère et al. 2015a, b), deposition of metals on the solid materials (Meng et al. 2018; Bozbag et al. 2012), extraction, food, cosmetics, pharmaceutics, materials, chemistry, sterilization, cleaning,

impregnation, formulation, energy, and waste treatment (Xu et al. 1999; Yuranov et al. 2003; Kim et al. 2008; Hayward et al. 2001; De Melo et al. 2014). Supercritical $CO_2$ deposition method, a green technique to prepare solid material supported metal nanoparticles, has taken significant attention for the last 20 years. The $scCO_2$ deposition technique is briefly described as the dissolution of the metal-organic precursor in the $scCO_2$, then the adsorption of the organometallic complex to the solid material surface, and finally the thermal (Bayrakceken et al. 2008) or chemical reduction (Bayrakceken et al. 2010) of the composite metal. Due to its high reduction properties, the most preferred reduction method that is thermal reduction is carried out in an inert atmosphere at atmospheric pressure or $scCO_2$. Another popular reduction method is a chemical reduction in $scCO_2$ or at atmospheric pressure with a reducing agent such as hydrogen or alcohol. The particle size of metallic nanoparticles obtained by chemical reduction is greater than that obtained by thermal reduction (Saquing et al. 2005; Sánchez-Miguel et al. 2017). It is known that in these processes, parameters such as time, temperature, pressure, and solubility of the precursor in each stage are fundamental to achieve catalyst with the appropriate properties. The solubility of the precursor in $scCO_2$ is a significant criterion for the preference of appropriate metal complexes. Because, the metal loading of support, the crystal structure of metal nanoparticles on the support, the particle size and distribution are depended to the solubility of the precursor in deposition conditions (Zhang and Erkey 2006; Aggarwal et al. 2013).

Palladium catalyst has received significant attention due to its application in industrially important areas such as hydrogenation, C-C cross-coupling reactions (Yılmaz and Güzel 2014; Yılmaz et al. 2017; Baran et al. 2018; Ghasemi and Karim 2018), oxidation reactions, and hydrogen storage (Erünal et al. 2018). In addition to being able to catalyze many reactions, palladium is a major issue, and the synthesis of organometallic compounds of palladium is quite simple, under favorable conditions. Besides, the availability of palladium as both homogeneous and heterogeneous catalyst brings ease of use. It has also taken an important place in nanocatalyst synthesis, where both homogeneous and heterogeneous catalyst systems are targeted.

The impregnation of Pd precursor via $scCO_2$ deposition on the SBA-15 was carried out at 40 °C under 8.5 MPa while the reduction was carried out at 40 °C under $H_2$ pressures at 60 bar (6 MPa) (Morère et al. 2011). Also, an additional thermal treatment was carried out after the reduction with hydrogen. In another study, impregnation of the Pd(0) complex on the SBA-15 surface was carried out at 41.4 MPa and 85 °C for 4 h. Owing to that complex used, no reduction is necessary after impregnation (Hunt et al. 2014). On the other hand, use of various co-solvents is another way to prepare dispersed nanoparticles by increasing the solubility of the precursor. Lee et al. dissolved the Pd precursor in THF and evaporate on the SBA-15 surface at 60 °C and 10 MPa for impregnation and then reduced to 80 °C at a pressure of 17.2 MPa with a $CO_2/H_2$ mixture (Lee et al. 2006). Besides, when $H_2$ reduction is used in $scCO_2$ deposition studies, relatively larger particle sizes are obtained if compared to thermal reduction. For example, Tenorio et al. reported 5.2–7.9 nm particle sizes with 30–50 nm length from their study which Pd impregnation was carried out at 40–80 °C under 8.5–14 MPa following $H_2$ reduction at 40 and 60 bar (6 MPa) $H_2$ pressure (Tenorio et al. 2012). The novelty of the current study is to achieve much smaller nanoparticles in length without the usage of co-solvent and still applying much lower temperature and $H_2$ pressure (80 °C under 1.03 MPa $H_2$ pressure, 17.2 MPa total pressure).

The fact that the temperature and $H_2$ pressure used are much lower (80 °C and 1.03 MPa) is a key novelty factor in our work. In addition, it is observed that the nanoparticles obtained in the $scCO_2$ deposition methods in which the hydrogen reduction step is used are mostly large. The impregnation of Pd precursor via $scCO_2$ deposition on the SBA-15 was carried out at 40–80 °C under 8.5–14 MPa while the reduction was carried out at 40 °C under $H_2$ pressures at 60 bar (6 MPa) (Tenorio et al. 2012). In this study, they reported particles 5–8 nm (limited by the pore size) and 30–50 nm long. But the long of the nanoparticles obtained in our study is much smaller than similar methods. In our study, we carried out the deposition process without adding the organic co-solvent.

In the $scCO_2$ deposition method, a limited number of precursors are used, and these precursors are cyclooctadiene, β-diketonate, dithiocarbamate, amine,

and their derivatives. These precursors are difficult to prepare, expensive, and sometimes require cosolvent during deposition because of low solubility. It also has disadvantages due to the high temperature (100–300 C) and pressure requirement during the deposition. We have contributed to the literature new precursor classes used for the green preparation of supported metallic nanoparticles in our previous studies. Pd (II) complexes of phenanthrenequinonedioxime and dimethylglyoxime ligands were synthesized by our group and used for deposition on alumina supports in the $scCO_2$ medium (Ulusal et al. 2017). Also, we synthesized Pd precursor with the perfluoroalkyl chain group and used for deposition on the MW-CNTs (Tezcan et al. 2018). Moreover, we carried out the deposition of bipyridyl and phenanthroline-derived Pd (II) complexes, which we designed as a new precursor class, on SBA-15 (Ulusal and Güzel 2018; Ulusal 2017) and MW-CNTs (Erünal et al. 2018) in the $scCO_2$ medium. In our previous work, we have shown that the palladium complex of 2,2′-bipyridyl can be an alternative to the precursors in the literature on the deposition technique in which chemical reduction is carried out with the help of hydrogen. It is particularly preferred because it is very easy to prepare in a short time like 15 min and is suitable for storage at low temperature and pressure. The small size of the molecule used means that there is a little steric hindrance between the molecules and that there is more Pd precursor at the surface during deposition. This helps to form more homogeneously dispersed Pd nanoparticles. A further advantage of the Pd (II) complex of 2,2′-bipyridyl is that according to the TGA result, a small energy of 78.42 J/g is required to separate the two bipyridyl molecules in the structure, and this allows the deposition to occur at lower temperatures and pressures. Also, the melting point of the precursor was found as 413.8 °C that temperature is very important for the $scCO_2$ deposition process. The relationship between the precursor melting point and the ideal solubility conditions used in the nanoparticle process by the SCFD method has been reported to be a major problem. Accordingly, if the precursor used is larger than the melting point of the temperature of the deposition conditions, large particles are formed and accordingly, low activity catalysts are obtained (Incera Garrido et al. 2008; Türk 2014; Türk and Erkey 2018). In this present paper, the effect of the precursor on the structure of nanoparticles inside and onside of SBA-15 porous was investigated. Mesoporous SBA-15-supported Pd nanoparticles were prepared with supercritical carbon dioxide ($scCO_2$) deposition method by $H_2$-assisted chemical reduction. For this aim, Pd (II) complexes of 2,2′-bipyridyl were used successfully for preparation of SBA-15-supported metallic Pd nanoparticles.

## Experimental

### Materials

2,2′bipyridyl was purchased from Sigma-Aldrich. Palladium (II) chloride used for precursor synthesis was supplied from ABCR GmbH. SBA-15 template silica (SBA-15) with mesoporous structure, < 150 μm particle size, pore size 6 nm, hexagonal pore morphology, which is used as solid support for deposition were obtained from Sigma-Aldrich with a purity of ≥ 99.9%. All chemicals were used without further purification.

### Solubility tests in supercritical carbon dioxide

Palladium (II) complex of 2,2′-bipyridyl was prepared to be used as a $scCO_2$ precursor according to the methodology given our previous research (Erünal et al. 2018). The solubility of bis(2,2′ bipyridyl) palladium (II) chloride precursor was tested for four different pressures as 10.3, 13.8, 17.2, and 20.7 MPa at 80 °C in the high-pressure reactor (sapphire window, 0.1 L). Approximately 150 mg of the complex was placed in the clear vessel. The vessel was warmed up to 80 °C and filled with $CO_2$ up to the desired pressures with a syringe pump. After obtaining saturated solutions, the saturated supercritical solution was taken to a 5-mL receptacle at the 80 °C. Then, the sample into the holder was transferred to 5 mL of ethanol in Schlenk tube. To finish the solubility test, the receptacle was washed with hot ethanol (~ 10 mL) for the purpose of removing the residual and added to the washing solution. Final ethanol solutions were tested with a Perkin Elmer Lambda 25 UV-Vis spectrophotometer for determination of solubility. The solubility tests of the complexes were repeated three times, and average solubility value was calculated.

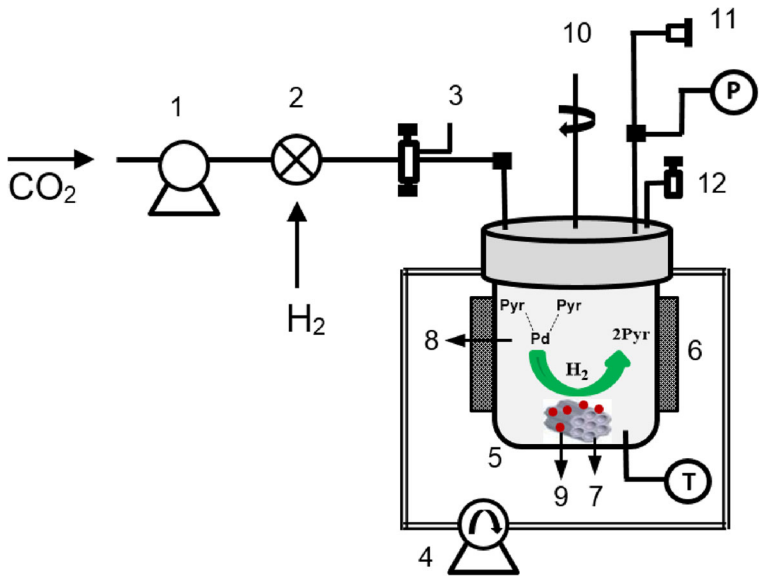


**Fig. 1** Schematic diagram of $scCO_2$ deposition system. (1) $CO_2$ syringe pump, (2) $H_2/CO_2$ mixing unit, (3) inlet valve, (4) water circulator for cooling, (5) vessel, (6) heating jacket, (7) SBA-15, (8) precursor, (9) nano-particle, (10) magnetic stirrer, (11) safety disc, (12) vent

## Green preparation of Pd/SBA-15 nanoparticles by $ScCO_2$ deposition method

Pd/SBA-15 samples were prepared by the hydrogen-assisted using supercritical deposition technique. A stainless steel high-pressure reactor with an internal volume of 54 mL was used for the deposition studies.

The deposition process was carried out in 3 steps: (1) dissolution of the precursor in $scCO_2$ under 17.2 MPa pressure and at 80 °C, (2) adsorption of the precursor on the surface of SBA-15 in same conditions, and (3) reduction of palladium complex to Pd(0) by $H_2$ gas. The schematic diagram of the high-pressure reactor used is given in Fig. 1.

Two hundred milligrams of SBA-15 and the precursor in the required amount of Pd were added in a high-pressure reactor with a window of sapphire glass. The expected theoretical Pd loading was 5.16% of the catalyst (That was calculated as the ratio of the mass of Pd to the total catalyst mass). In order to completely remove the oxygen in the vessel, it was pre-treated with $CO_2$ for 1 h. During the first step, the reactor was gradually heated up to 80 °C with a circulating heater/cooler and was then filled with 17.2 MPa $CO_2$ gas with a syringe pump (Isco 260D). After the system was allowed to be saturated for 1 h under these conditions, the gas in the reactor was evacuated and the gas pressure was reduced to 10.3 MPa. Then, 23 mmol $H_2$ gas and $CO_2$ gases (with a total pressure of 17.2 MPa) in a 10-mL intermediate volume were transferred to the system. Finally, the reactor was pressurized at 17.2 MPa with a syringe pump and stirred under these conditions for 24 h. At

**Table 1** Experimental data for the solubility (S) of the investigated precursor in $scCO_2$ at different pressures and densities (kg $m^{-3}$)

| Substance | S (×10 $^{4}$ mol/L) | | | | | | |
|---|---|---|---|---|---|---|---|
| | 235.6[a]/10.3[b] | 337[a]/13.8[b] | 377[a]/13.8[b] | 501.7 [a]/17.2[b] | 551[a]/20.7[b] | 606.8 [a]/20.7[b] | 672[a]/27.6[b] |
| $PdPyr_2Cl_2$[c] | 0.612 | | 2.653 | 3.877 | | 5.713 | |
| $PdPhenCl_2$[c] | 0.605 | | 3.170 | 5.199 | | 6.454 | |
| Pd $(PTQD)_2$[d] | | 1.991 | | | 4.959 | | 8.171 |
| Pd $(DMG)_2$[d] | | 2.681 | | | 7.138 | | 10.691 |

[a] $\rho$ (kg $m^{-3}$ )
[b] P (MPa)
[c] 80 °C, [d] 90 °C

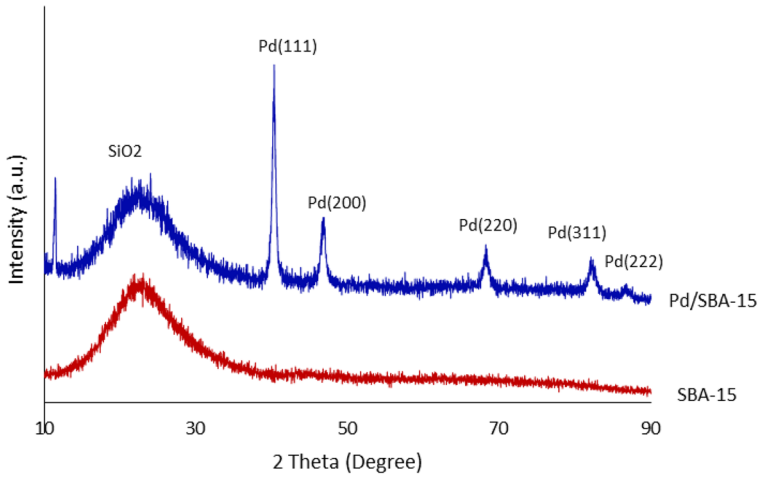


**Fig. 2** XRD result of SBA-15 and SBA-15-supported Pd nanoparticles. The nanoparticle size is calculated as 16.2 nm

the end of this period, the system was brought to room temperature and the gas inside was slowly discharged. The obtained gray Pd/SBA-15 nanoparticles (catalyst) were washed with ethanol and dried in an 80 °C oven. The quantitative amount of total palladium in the prepared catalyst was quantified by ICP-OES (Perkin Elmer 2100 DV). HR_TEM (Jeol 2100F HR_TEM) was used for analyzing the surface morphology. Particle

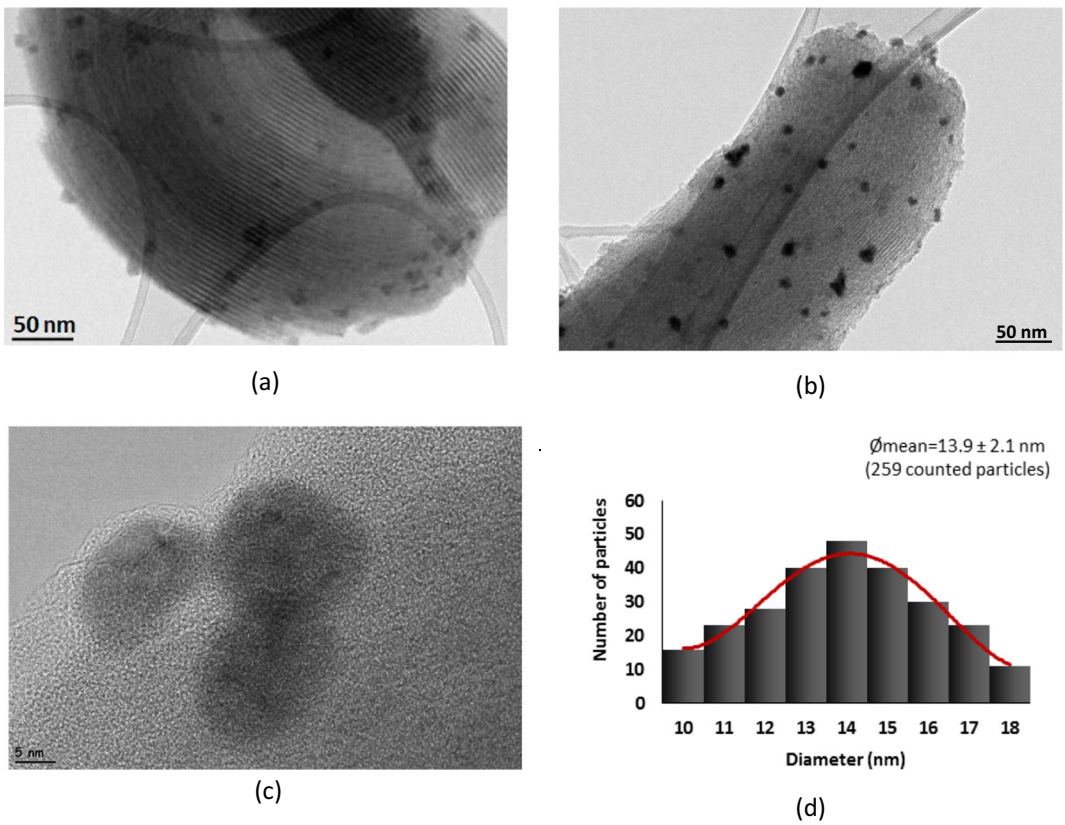


**Fig. 3** HR-TEM images and particle size distribution of SBA-15-supported Pd nanoparticles. The gray background is corresponding to SBA-15 support while black dots on the gray background are Pd nanoparticles. Pd nanoparticles have a homogeneous dispersion with any agglomeration. **a**, **b** 50 nm. **c** 5 nm. **d** The size distribution of Pd nanoparticles: the mean diameter of 259 particles is 13.9 ± 2.1 nm

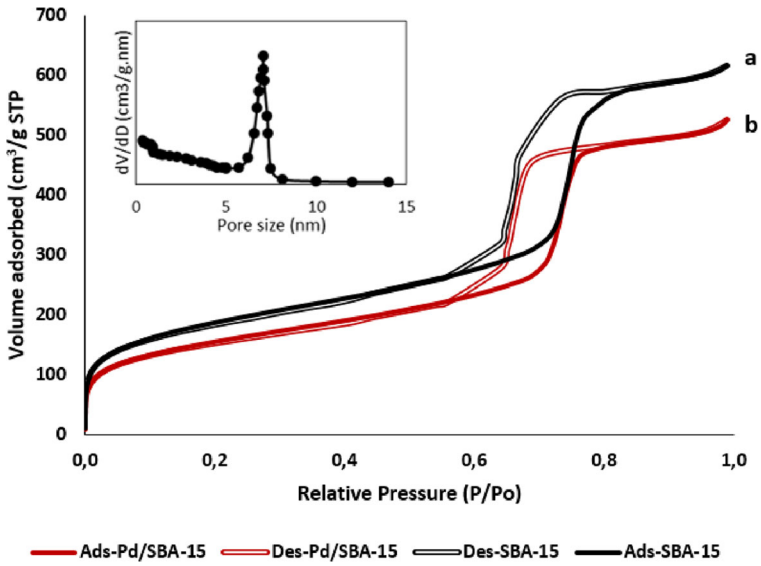


**Fig. 4** Nitrogen adsorption–desorption isotherms of **a** SBA-15 and **b** SBA-15-supported Pd catalyst at 77.4 K. (Inset: pore size distributions of the corresponding samples from adsorption branch)

size and crystal structure were analyzed by XRD (Rigaku Miniflex, CuKα, λ = 0.154 nm). A Micromeritics Tristar II 3020 instrument was used to analyze the surface areas and pore properties $N_2$ adsorption–desorption isotherms recorded at 77.4 K. The pure support and catalyst were degassed at 300 K for 3 h under vacuum before treatment. The Brunauer–Emmett–Teller (BET) equation was used to calculate the specific surface areas. Pore volume and pore size were determined with the Barrett–Joyner–Halenda (BJH) model, and the adsorption branches of nitrogen physisorption isotherms were used to calculate the pore size and pore volume. X-ray photoelectron spectroscopy (XPS) measurements were performed in Thermo Scientific Al K-Alpha.

### Catalytic tests

The Suzuki–Miyaura C-C cross-coupling reaction of a phenylboronic acid and bromobenzene at room temperature was chosen as a model reaction to test the catalytic performance of prepared Pd/SBA-15 nanoparticles. In these reactions, triethylamine, which is an organic base, and $K_2CO_3$ and NaOH, which are inorganic bases, are used as bases.

An Agilent 6850 Gas Chromatography (GC) instrument was used to calculate the reaction efficiency. Before analysis by GC, the products were extracted and purified from the column containing silica gel and anhydrous $Na_2SO_4$.

## Results and discussion

### The solubility of precursor in $ScCO_2$

The solubility results were evaluated in the $scCO_2$ medium, and the highest resolution condition was selected as the deposition conditions for 80 °C and 20.7 MPa pressure. The solubilities of the present precursor ($PdPyr_2Cl_2$) and our other precursor (Ulusal et al. 2017; Ulusal and Güzel 2018) in previous studies at different pressures and densities are shown in Table 1.

It was found that fluorinated complexes have a high solubility compared with the corresponding non-fluorinated complexes. Alkyl groups in the ligands

**Table 2** Textural properties of SBA-15 and Pd/SBA-15 catalyst

| Substrate | $S_{BET}$ ($m^2$/g) | Average pore diameter, BJH (nm) | $V_p$ ($cm^3$/g) |
|---|---|---|---|
| SBA-15 | 647.2 | 3.7 | 0.97 |
| Pd/SBA-15 | 492.6 | 3.8 | 0.76 |

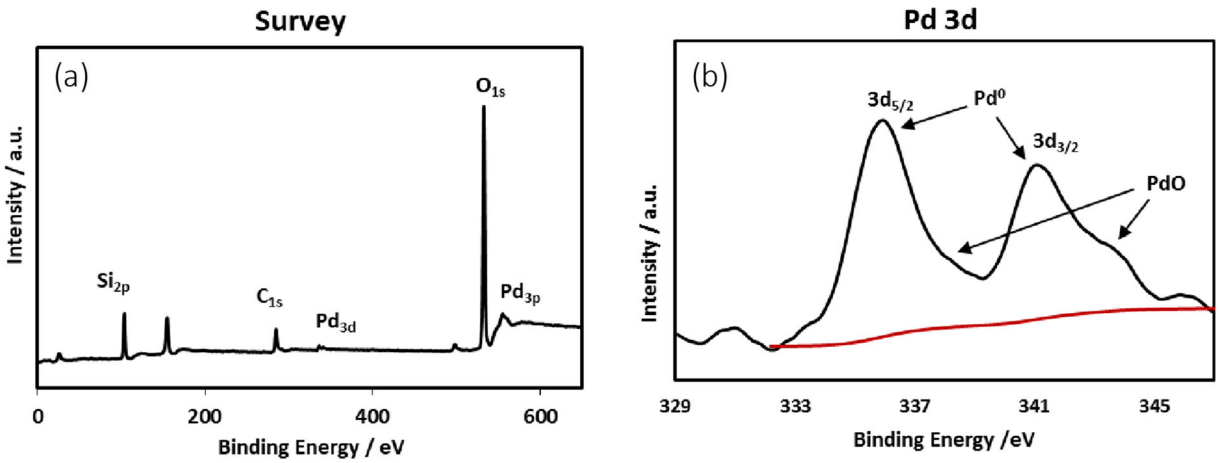


**Fig. 5** Survey XPS spectrum of Pd/SBA-15 nanoparticles (**a**). High-resolution XPS spectra of Pd3d (**b**) orbitals

enhance the solubility of the complex. On the other hand, aryl groups lead to a lower solubility (Aschenbrenner et al. 2007). So, we expect that the solubility of $PdPyr_2Cl_2$ in $scCO_2$ is similar to the used precursor in literature. It is concluded that the solubility of $PdPyr_2Cl_2$ is similar to the solubility of $PdPhenCl_2$ which we used in our previous studies.

## Characterization of Pd/SBA-15

The amount of total Pd in the catalyst was determined around 5.0% by ICP-OES measurements. The catalyst was prepared according to the theoretical Pd loading around 5.16%. From the obtained data, the deposition efficiency was found as 96.9%.

To analyze the size and crystal structure of the catalyst, XRD measurement was performed. The wide-angle XRD pattern of SBA-15 and Pd/SBA-15 is shown in Fig. 2. Amorphous $SiO_2$ support peak appeared 2θ degrees of ca. 23° with a shallow and very board reflection (JCPDS card number is 01-086-1561). The presence of very intensive sharp peaks observed at 2θ = 40.29 ° assigned to (111), 2θ = 46.87 ° assigned to (200), 2θ = 68.18 ° assigned to (220), and 2θ = 82.6 ° assigned to (311) reflections of the face-centered cubic Pd lattice system, with the space group referred to Fm-3m (JCPDS card number is 46-1043). Pd peaks indicated that particles are very small. Pd nanoparticle size was calculated via the Scherrer equation as 13.7 nm due (111) peak.

HR-TEM images of pure SBA-15 and Pd/SBA-15 are shown in Fig. 3. The dark nanoparticles are homogeneously distributed on the surface of the SBA-15 with the gray-colored parallel channel. It can be seen from Fig. 3a, b that the resulting Pd nanocatalysts are mostly deposited both on the exterior surface of the support and between its channels. It can be estimated that the nanoparticles forming in the channels are larger than those formed on the surface and distributed over a wider surface. The particles are dispersed homogeneously on the support without agglomeration on the surface. Although some of the Pd nanoparticles on the surface of SBA-15 are very small, some of them are together (it can be seen from Fig. 3c). Despite the possibility of Pd nanoparticles forming in the SBA-15 pores, there is no definite conclusion in this regard as there is no image from the pores. However, it can be said that this probability is very low because the particle size obtained from XRD is larger than the pores (Liu et al. 2008). The mean particle size diameters were calculated as 13.9 ± 2.1 nm that also supports XRD data.

The porosities of SBA-15 and Pd/SBA-15 were further studied by $N_2$ adsorption–desorption isotherms. $N_2$ adsorption–desorption isotherms of support and catalyst can be seen in Fig. 4. These two obtained isotherms exhibit a type IV which is a characteristic isotherm of mesoporous materials such as SBA-15 and MCM-41 according to the IUPAC classification. Table 2 shows textural properties (BET surface area ($S_{BET}$), pore size and pore volume (Vp)) obtained from these isotherms (Al-Othman 2012). BET surface area of SBA-15 was 647.2 $m^2/g$, total pore volume was 0.97 $cm^3/g$, and the pore diameter was 3.7 nm. After deposition of Pd on the SBA-15, BET surface area was 492.6 $m^2/g$, total pore volume was 0.76 $cm^3/g$, and pore diameter was 3.8 nm. Adsorption isotherm of Pd/SBA-15 is very similar to the

**Table 3.** Suzuki-Miyaura Cross-Coupling Reactions of phenylboronic acid and bromobenzene via SCF deposited Pd/SBA-15

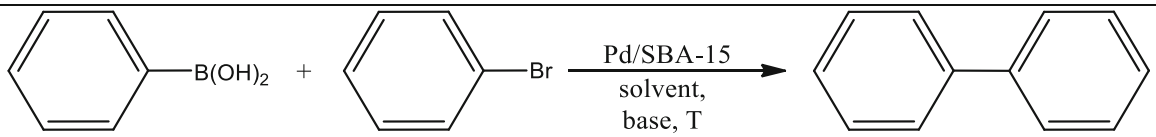


Phenylboronic acid bromobenzene biphenyl

| Exp. No. | Catalyst | Base | Solvent | T (°C) | t (h) | Yield (%)* | TON |
|---|---|---|---|---|---|---|---|
| **1** | Pd/SBA-15 | $K_2CO_3$ | Ethanol | 30 | 24 | 80.4 | 160.8 |
| **2** | Pd/SBA-15 | $K_2CO_3$ | Methanol | 30 | 24 | 13.1 | 26.2 |
| **3** | Pd/SBA-15 | $K_2CO_3$ | NMP | 30 | 24 | 43.8 | 87.6 |
| **4** | Pd/SBA-15 | $K_2CO_3$ | DMF | 30 | 24 | 37.5 | 75 |
| **5** | Pd/SBA-15 | $K_2CO_3$ | Acetonitrile | 30 | 24 | 31.2 | 62.4 |
| **6** | Pd/SBA-15 | $K_2CO_3$ | Dioxane | 30 | 24 | 33.6 | 67.2 |
| **7** | Pd/SBA-15 | NaOH | Ethanol | 30 | 24 | 52.2 | 104.4 |
| **8** | Pd/SBA-15 | NaOH | Methanol | 30 | 24 | 12.9 | 25.8 |
| **9** | Pd/SBA-15 | NaOH | NMP | 30 | 24 | 42.2 | 84.4 |
| **10** | Pd/SBA-15 | NaOH | DMF | 30 | 24 | 11.3 | 22.6 |
| **11** | Pd/SBA-15 | NaOH | Acetonitrile | 30 | 24 | 18.2 | 36.4 |
| **12** | Pd/SBA-15 | NaOH | Dioxane | 30 | 24 | 34.8 | 69.6 |
| **13** | Pd/SBA-15 | $Et_3N$ | Ethanol | 30 | 24 | 31.9 | 63.8 |
| **14** | Pd/SBA-15 | $Et_3N$ | Methanol | 30 | 24 | 6.6 | 13.2 |
| **15** | Pd/SBA-15 | $Et_3N$ | NMP | 30 | 24 | 11.4 | 22.8 |
| **16** | Pd/SBA-15 | $Et_3N$ | DMF | 30 | 24 | 10.9 | 21.8 |
| **17** | Pd/SBA-15 | $Et_3N$ | Acetonitrile | 30 | 24 | 3.6 | 7.2 |
| **18** | Pd/SBA-15 | $Et_3N$ | Dioxane | 30 | 24 | 21.1 | 42 |
| **19** | Pd/SBA-15 | $K_2CO_3$ | Ethanol | 60 | 1.5 | 100 | 200 |
| **20** | Pd/SBA-15 | $K_2CO_3$ | Ethanol | 80 | 0.5 | 100 | 200 |

**Reaction ingredient: Pd (0.0050 mmol), bromobenzene (1.0 mmol), phenylboronic acid (1.20 mmol), base (2.0 mmol), organic solvent (2.0 ml) and water (2.0 ml)**
*** Isolated yields**
**TON (Turnover number of catalyst): moles of bromobenzene converted per mole of Pd.**

Reaction ingredient: Pd (0.0050 mmol), bromobenzene (1.0 mmol), phenylboronic acid (1.20 mmol), base (2.0 mmol), organic solvent (2.0 ml) and water (2.0 ml)
* Isolated yields
*TON* (Turnover number of catalyst): moles of bromobenzene converted per mole of Pd.

support; as a result, it can be said that metal addition on the support does not affect the porous structure (Morère et al. 2015a, b; Matei et al. 2016; Duan et al. 2017), but the amount of adsorbed nitrogen is decreased. Both SBA-15 and Pd/SBA-15 isotherms exhibit a sharp capillary condensation step in the $P/P_0$ range of 0.6–0.8 dissociation between 0.6 and 0.8. This is an indication of the uniformity of the pore sizes (Wang and Liu 2011). When the hysteresis loops of SBA-15 and Pd/SBA-15 analyzed, it can be said that palladium loading makes the hysteresis smaller with decreasing surface area, total pore volume, and increasing pore diameter. The decreases of surface area could be due to the incorporation of Pd nanoparticles into the pores of SBA-15 and/or the block by the Pd nanoparticles (Yao et al. 2015). Total pore volume of Pd/SBA-15 demonstrate an average shift of 0.21 $cm^3/g$ with palladium loading. It can be said that the slight increase in pore size can be explained as a cause with Pd inclusion.

X-ray photoelectron spectroscopy analysis of Pd/SBA-15 is shown in Fig. 5 (Pd3d). XPS analyses were used to specify the chemical state of palladium in the catalyst.

**Table 4** Comparison between catalytic performances of mesoporous silica-supported palladium nanocatalyst and different catalysts in the Suzuki–Miyaura cross-coupling reactions

| Catalyst | Yield(%) | Time | Temp. (°C) | Solvent | TON | Base | Reference |
|---|---|---|---|---|---|---|---|
| Pd/SBA-15 | 21 | 0.5 h | 100 | Ethanol | Unvalued | $K_3PO_4$ | Zheng et al. (2010) |
| Pd/dendrimer | 97 | 20 h | 101 (Reflux) | 1,4-dioxane | Unvalued | $K_3PO_4$ | Wu et al. (2006) |
| Pd/SBA-15 | 80.2 | 3 h | 110 | Ethanol | 1360 | $Et_3N$ | Ncube et al. (2015) |
| Pd/SBA-15 | 90 | 6 h | 90 | Ethanol | 900 | $K_2CO_3$ | Sarkar et al. (2015) |
| Pd/SBA-15 | 80.4 | 24 h | Room temp. | Ethanol | 160.8 | $K_2CO_3$ | Present study |
| Pd/SBA-15 | 100 | 1.5 h | 60 | Ethanol | 200 | $K_2CO_3$ | Present study |

Metallic palladium (Pd0) was observed with two characteristic peaks that correspond to Pd $3d_{3/2}$ (336.08 eV) and Pd $3d_{5/2}$ (341.28 eV) which is in agreement with literature data (Duan et al. 2017). These results show that palladium is in metallic form in the catalyst verifying the XRD data. Since metallic palladium is more active than palladium oxide in the heterogeneous catalyst, the activity of the catalyst is expected to be high for the coupling reaction. On the other hand, the peaks of the high-resolution XPS spectrum ($Si_{2p}$, $C_{1s}$, $Pd_{3d}$, $O_{3s,}$ and $Pd_{3p}$) are provided in Fig. 5 (Survey). Moreover, the absence of Cl peaks in the catalyst supports the complete removal of the ligands from the catalyst.

## Application of Pd/SBA-15 as a catalyst in Suzuki–Miyaura cross-coupling reaction

The catalytic performance of 0.5 mol% Pd/SBA-15 was assessed for Suzuki–Miyaura cross-coupling reaction of bromobenzene and phenylboronic acid at room temperature under atmospheric conditions. Even though there are many studies about Pd-catalyzed Suzuki–Miyaura cross-coupling reaction of Pd (0) and Pd (II) on the various supports, room temperature conditions are not satisfactory for many of them. In order to find the optimum conditions for the prepared catalyst, it was tested in six different solutions (2.0 mL) of ethanol, methanol, DMF, NMP, acetonitrile, and 1,4-dioxane. The influence of organic and inorganic bases (2.0 mmol), $K_2CO_3$, NaOH, and triethylamine were also investigated during the reactions. The obtained results are summarized in Table 3.

Heterogeneous Pd nanoparticles generally need high temperatures 100–120 °C in Suzuki–Miyaura reactions because of the high activation energy in mechanism steps (Li et al. 2013; Molnar 2011; Dumbre et al. 2016). Reaction temperature rise increases the product yield automatically.

Turnover number of catalyst (TON) was calculated as moles of desired product formed/number of total catalyst. To calculate the TON value, the amount of Pd

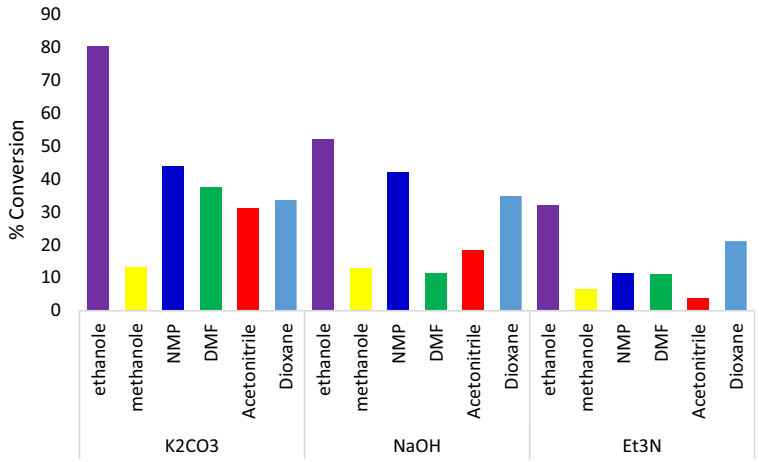


**Fig. 6** Catalytic performance of Pd/SBA-15 in different solvents and bases

**Table 5.** Pd/SBA-15 recycles study in Suzuki reaction

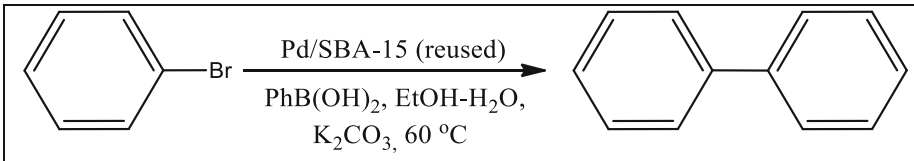


| Run | Yield (%) |
|---|---|
| **1** | 100 |
| **2** | 98 |
| **3** | 96 |
| **4** | 90 |
| **5** | 83 |
| **6** | 70 |
| **7** | 52 |

Reaction ingredient: Pd (0.0050 mmol), bromobenzene (1.0 mmol), phenylboronic acid (1.20 mmol), $K_2CO_3$ (2.0 mmol), ethanol (2.0 ml) and water (2.0 ml), 24 h

in the Pd/SBA-15 was determined by ICP-OES. The calculated TON results obtained are given in Table 3. Although the TON values are quite high for a heterogeneous catalyst, the highest value was found as 160.8 in the ethanol-$K_2CO_3$ pair. It can be said that the nanocatalyst prepared when the TON values are compared with the literature has high efficiency (given in Table 4).

The reaction conversion graphs in different solvents and bases are given in Fig. 6. In general, $K_2CO_3$, which is an inorganic base for virtually all used solvents, appears to have the best results when examining the effect of the bases when the solvents are held constant. For each of the 3 bases used, the highest catalytic activity was reached as the result of the solvent system being ethanol/water. The highest catalytic conversion was obtained in the ethanol-$K_2CO_3$ solvent-base pair. Also, it is clear that the solvent-base pair with the lowest conversion is $Et_3N$-acetonitrile. The catalyst shows higher yields at lower temperatures than many catalysts in the literature. Table 4 shows the comparison of our catalyst and the catalytic activities of other catalysts in the literature. As seen in the table, although the Suzuki reaction is usually carried out above 50 °C, our catalyst exhibits high activity at room temperature. When the literature given in Table 4 is examined, the catalytic activity results at room temperature show high activity at much lower temperatures than similar reactions. Also, according to the activity results at 60 °C, 100% efficiency was obtained in as short as 1.5 h.

The lifetime of Pd/SBA-15 catalyst at 60 °C with the same reaction conditions were also tested. The results were given in Table 5. It is seen that the catalyst can be reused four times without a significant decrease in catalytic activity under these conditions.

## Conclusions

The deposition of Pd nanoparticles on SBA-15 templated mesoporous silica was successfully carried out using synthesized Pd (II) complex of 2,2′bipyridyl as a precursor in supercritical carbon dioxide under mild conditions. Prepared SBA-15-supported Pd nanoparticles were used to catalyze Suzuki–Miyaura cross-coupling reaction of a phenylboronic acid and bromobenzene at room temperature. Moreover, homogeneously well-dispersed metallic palladium nanostructures were obtained with particles 13.7 nm determined from XRD. Palladium was in metallic form in the catalyst according to XPS results. It was found that Pd loading is very high according to nanoparticles prepared with similar methods. The catalytic activities at room temperature of Pd/SBA-15 were tested in various organic solvent:water (1:1) ethanol, methanol, NMP, DMF, 1,4-dioxane, and acetonitrile with the different bases

$K_2CO_3$, NaOH, and $Et_3N$, separately. The best catalytic activity was obtained in the reaction using ethanol/water solution and $K_2CO_3$ base at room temperature, and its TON value was 160.8 which is better than many catalysts in literature. Catalyst re-usability was achieved at 60 °C and activity was found to continue to a significant extent at 4 uses.

**Acknowledgments** We gratefully acknowledge Prof. Dr. Ramazan Esen and Merhan Kılıç from Physics Department of Cukurova University for the XRD measurements, Prof. Dr. Deniz Uner and Atalay Çalışan from Chemical Engineering Department of Middle East Technical University for the BET analysis, and Etkin Barış Çetin from Department of Metallurgical and Materials Engineering of Dokuz Eylül Universty for the XPS analysis.

**Funding information** This study was funded by the Management Unit of Scientific Research Projects of Çukurova University (BAP project no: FDK-2015-3668 under thesis). Dr. Fatma Ulusal has received research grants from Scientific and Technological Research Council of Turkey (BIDEB 2211-E domestic graduate scholarship program).

**Compliance with ethical standards**

**Conflict of interest** The authors declare that they have no conflict of interest.

## References

Aggarwal V, Reichenbach LF, Enders M, Muller T, Wolff S, Crone M, Türk M, Brase S (2013) Influence of perfluorinated end groups on the SFRD of [Pt (cod) me (CnF2n+1)] onto porous Al2O3 in CO2 under reductive conditions. Chem Eur J 19: 12794–12799. https://doi.org/10.1002/chem.201301191

Al-Othman ZA (2012) A review: fundamental aspects of silicate mesoporous materials. Materials 5:2874–2902. https://doi.org/10.3390/ma5122874

Aschenbrenner O, Kemper S, Dahmen N, Schaber K, Dinjus E (2007) Solubility of β-diketonates, cyclopentadienyls, and cyclooctadiene complexes with various metals in supercritical carbon dioxide. J Supercrit Fluids 41:179–186. https://doi.org/10.1016/j.supflu.2006.10.011

Baran NY, Baran T, Menteş A (2018) Production of novel palladium nanocatalyst stabilized with sustainable chitosan/cellulose composite and its catalytic performance in Suzuki-Miyaura coupling reactions. Carbohydr Polym 181:596–604. https://doi.org/10.1016/j.carbpol.2017.11.107

Bayrakceken A, Smirnova A, Kitkamthorn U, Aindow M, Turker L, Eroglu I, Erkey C (2008) Pt-based electrocatalysts for polymer electrolyte membrane fuel cells prepared by supercritical deposition technique. J Power Sources 179:532–540. https://doi.org/10.1016/j.jpowsour.2007.12.086

Bayrakceken A, Cangul B, Zhang LC, Aindow M, Erkey C (2010) PtPd/BP2000 electrocatalysts prepared by sequential supercritical carbon dioxide deposition. Int J Hydrog Energy 35: 11669–11680. https://doi.org/10.1016/j.ijhydene.2010.08.059

Beckman EJ (2004) Supercritical and near-critical CO2 in green chemical synthesis and processing. J Supercrit Fluids 28: 121–191. https://doi.org/10.1016/S0896-8446(03)00029-9

Bozbag SE, Kostenko SO, Kurykin MA, Khrustalev VN, Khokhlov AR, Zhang L, Aindow M, Erkey C (2012) Aerogel–copper nanocomposites prepared using the adsorption of a polyfluorinated complex from supercritical CO2. J Nanopart Res 14:973. https://doi.org/10.1007/s11051-012-0973-7

De Melo MMR, Silvestre AJD, Silva CM (2014) Supercritical fluid extraction of vegetable matrices applications, trends and future perspectives of a convincing green technology. J Supercrit Fluids 92:115–176. https://doi.org/10.1016/j.supflu.2014.04.007

Duan Y, Zheng M, Li D, Deng D, Wu C, Yang Y (2017) Synthesis of Pd/SBA-15 catalyst employing surface-bonded vinyl as a reductant and its application in the hydrogenation of nitroarenes. RSC Adv 7:3443–3449. https://doi.org/10.1039/c6ra26811k

Dumbre D, Choudhary VR, Selvakannan PR (2016) Cu–Fe layered double hydroxide derived mixed metal oxide: environmentally benign catalyst for Ullmann coupling of aryl halides. Polyhedron 120:180–184. https://doi.org/10.1016/j.poly.2016.09.052

Erünal E, Ulusal F, Aslan MY, Güzel B, Üner D (2018) Enhancement of hydrogen storage capacity of multi-walled carbon nanotubes with palladium doping prepared through supercritical CO2 deposition method. Int J Hydrog Energy 43:10755–10764. https://doi.org/10.1016/j.ijhydene.2017.12.058

Gang Z, Jiang HF, Chen MC (2003) Chemical reactions in supercritical carbon dioxide. Arkivoc 2003:191–198. https://doi.org/10.3998/ark.5550190.0004.222

Ghasemi S, Karim S (2018) Controlled synthesis of modified polyacrylamide grafted nano-sized silica supported Pd nanoparticles via RAFT polymerization through "grafting to" approach: application to the heck reaction. Colloid Polym Sci 296:1323–1332. https://doi.org/10.1007/s00396-018-4349-0

Hayward RC, Alberius-Henning P, Chmelka BF, Stucky GD (2001) The current role of mesostructures in composite materials and device fabrication. Microporous Mesoporous Mater 44(45):619–624. https://doi.org/10.1016/S1387-1811(01)00242-6

Hiramatsu M, Hori M (2010) Preparation of dispersed platinum nanoparticles on a carbon nanostructured surface using supercritical fluid chemical deposition. Materials 3:1559–1572. https://doi.org/10.3390/ma3031559

Hunt AJ, Budarin VL, Comerford JW, Parker HL, Lazarov VK, Breeden SW, Macquarrie DJ, Clark JH (2014) Deposition of palladium nanoparticles in SBA-15 templated silica using supercritical carbon dioxide. Mater Lett 116:408–411. https://doi.org/10.1016/j.matlet.2013.11.075

Incera Garrido G, Patcas FC, Upper G, Türk M, Yilmaz S, Kraushaar-Czarnetzki B (2008) Supercritical deposition of Pt on SnO2-coated Al2O3 foams: phase behaviour and

catalytic performance. Appl Catal A Gen 338:58–65. https://doi.org/10.1016/j.apcata.2007.12.019

Kim J, Kelly MJ, Lamb HH, Roberts GW, Kiserow DJ (2008) Characterization of palladium (Pd) on alumina catalysts prepared using liquid carbon dioxide. J Phys Chem C 112: 10446–10452. https://doi.org/10.1021/jp711495n

Lee SS, Park BK, Byeon SH, Chang F, Kim H (2006) Mesoporous silica-supported Pd nanoparticles; highly selective catalyst for hydrogenation of olefins in supercritical carbon dioxide. Chem Mater 18:5631–5633. https://doi.org/10.1021/cm061060s

Li XH, Baar M, Blechert S, Antonietti M (2013) Facilitating room-temperature Suzuki coupling reaction with light: Mott-Schottky photocatalyst for C-C-coupling. Sci Rep 3:1743. https://doi.org/10.1038/srep01743

Liu Y, Zhang J, Hou W, Jie Zhu J (2008) A Pd/SBA-15 composite: synthesis, characterization and protein biosensing. Nanotechnology 19:135707. https://doi.org/10.1088/0957-4484/19/13/135707

Matei D, Doicin B, Cursaru DL (2016) Pd/SBA-15 mesoporous catalyst for ethanol steam reformıng. A neural network approach. Dig J Nanomater Biostruct 11:443–451

Meng Y, Su F, Chen Y (2018) Effective lubricant additive of nano-Ag/MWCNTs nanocomposite produced by supercritical CO2 synthesis. Tribol Int 118:180–188. https://doi.org/10.1016/j.triboint.2017.09.037

Molnar A (2011) Efficient, selective, and recyclable palladium catalysts in carbon-carbon coupling reactions. Chem Rev 111:2251–2320. https://doi.org/10.1021/cr100355b

Morère J, Tenorio MJ, Torralvo MJ, Pando C, Renuncio JAR, Cabanas A (2011) Deposition of Pd into mesoporous silica SBA-15 using supercritical carbon dioxide. J Supercrit Fluids 56:213–222. https://doi.org/10.1016/j.supflu.2010.12.012

Morère J, Royuela S, Asensio G, Palomino P, Enciso E, Pando C, Cabañas A (2015a) Deposition of Ni nanoparticles onto porous supports using supercritical CO2: effect of the precursor and reduction methodology. Phil Trans R Soc A 373: 20150014. https://doi.org/10.1098/rsta.2015.0014

Morère J, Torralvo MJ, Pando C, Renuncio JAR, Cabanas A (2015b) Supercritical fluid deposition of Ru nanoparticles onto SiO2 SBA-15 as a sustainable method to prepare selective hydrogenation catalysts. RSC Adv 5:38880–38891. https://doi.org/10.1039/C5RA04969E

Ncube P, Hlabathe T, Meijboom R (2015) Palladium nanoparticles supported on mesoporous silica as efficient and recyclable heterogenous nanocatalysts for the Suzuki C–C coupling reaction. Appl Organomet Chem 29:517–523. https://doi.org/10.1007/s10876-015-0885-7

Sánchez-Miguel E, Tenorio MJ, Morère J, Cabañas A (2017) Green preparation of PtRu and PtCu/SBA-15 catalysts using supercritical CO2. J CO2 Util 22:382–391. https://doi.org/10.1016/j.jcou.2017.10.018

Saquing CD, Kang D, Aindow M, Erkey C (2005) Investigation of the supercritical deposition of platinum nanoparticles into carbon aerogels. Microporous Mesoporous Mater 80:11–23. https://doi.org/10.1016/j.micromeso.2004.11.019

Sarkar SM, Rahman ML, Yusoff MM (2015) Highly active thiol-functionalized sba-15 supported palladium catalyst for Sonogashira and Suzuki-Miyaura cross-coupling reactions. RSC Adv 5:1295–1300. https://doi.org/10.1039/C4RA13322F

Tenorio MJ, Pando C, Renuncio JAR, Stevens JG, Bourne RA, Poliakoff M, Cabañas A (2012) Adsorption of Pd (hfac)2 on mesoporous silica SBA-15 using supercritical CO2 and its role in the performance of Pd–SiO2 catalyst. J Supercrit Fluids 69:21–28. https://doi.org/10.1016/j.supflu.2012.05.003

Tezcan B, Ulusal F, Eğitmen E, Güzel B (2018) Preparation of metallic Pd nanoparticles using supercritical CO2 deposition: an efficient catalyst for Suzuki cross-coupling reaction. J Nanopart Res 20:145. https://doi.org/10.1007/s11051-018-4252-0

Türk M (2014) Particle formation with supercritical fluids. Elsevier, Amsterdam

Türk M, Erkey C (2018) Synthesis of supported nanoparticles in supercritical fuids by supercritical fluid reactive deposition: current state, further perspectives and needs. J Supercrit Fluids 134:176–183. https://doi.org/10.1016/j.supu.2017.12.010

Ulusal F (2017) The synthesis of precursors used in supercritical fluid deposition techniques and effect of precursors on particle morphology. Çukurova University, Adana

Ulusal F, Güzel B (2018) Deposition of palladium by the hydrogen assisted on SBA-15 with a new precursor using supercritical carbon dioxide. J Supercrit Fluids 133:233–238. https://doi.org/10.1016/j.supflu.2017.10.023

Ulusal H, Fındıkkıran G, Demirkol O, Akbaşlar D, Giray ES (2015) Supercritical diethylether: a novel solvent for the synthesis of aryl-3,4,5,6,7,9-hexahydroxanthene-1,8-diones. J Supercrit Fluids 105:146. https://doi.org/10.1016/j.supflu.2014.12.020

Ulusal F, Darendeli B, Erünal E, Eğitmen A, Güzel B (2017) Supercritical carbondioxide deposition of γ-alumina supported Pd nanocatalysts with new precursors and using on Suzuki-Miyaura coupling reactions. J Supercrit Fluids 127: 111–120. https://doi.org/10.1016/j.supflu.2017.03.024

Wang H, Liu C (2011) Preparation and characterization of SBA-15 supported Pd catalyst for CO oxidation. Appl Catal B 106: 672–680. https://doi.org/10.1016/j.apcatb.2011.06.034

Wu L, Li BL, Huang YY, Zhou HF, He YM, Fan QH (2006) Phosphine dendrimer-stabilized palladium nanoparticles, a highly active and recyclable catalyst for the Suzuki-Miyaura reaction and hydrogenation. Org Lett 8:3605–3608. https://doi.org/10.1021/ol0614424

Xu CL, Wei BQ, Ma RZ, Liang J, Ma XK, Wu DH (1999) Fabrication of aluminum–carbon nanotube composites and their electrical properties. Carbon 37:855–858. https://doi.org/10.1016/S0008-6223(98)00285-1

Yao Q, Lu ZH, Yang K, Chen X, Zhu M (2015) Ruthenium nanoparticles confined in SBA-15 as highly efficient catalyst for hydrolytic dehydrogenation of ammonia borane and hydrazine borane. Sci Rep 5:15186. https://doi.org/10.1038/srep15186

Yılmaz MK, Güzel B (2014) Iminophosphine palladium (II) complexes: synthesis, characterization, and application in heck cross-coupling reaction of aryl bromides. Appl Organomet Chem 28:529–536. https://doi.org/10.1002/aoc.3158

Yılmaz MK, Keleş H, Ince S, Keleş M (2017) Iminophosphine palladium catalysts for Suzuki carbonylative coupling reaction. Appl Organomet Chem 32. https://doi.org/10.1002/aoc.4002

Yuranov I, Moeckli P, Suvorova E, Buffat P, Kiwi-Minsker L, Renken A (2003) Pd/SiO2 catalysts: synthesis of Pd nanoparticles with the controlled size in mesoporous silicas. J Mol Catal A Chem 192:239–251. https://doi.org/10.1016/S1381-1169(02)00441-7

Zhang Y, Erkey C (2006) Preparation of supported metallic nanoparticles using supercritical fluids: a review. J Supercrit Fluids 38:252–267. https://doi.org/10.1016/j.supflu.2006.03.021

Zheng Z, Li H, Liu T, Cao R (2010) Monodisperse noble metal nanoparticles stabilized in SBA-15: synthesis, characterization and application in microwave-assisted Suzuki–Miyaura coupling reaction. J Catal 270:268–274. https://doi.org/10.1016/j.jcat.2010.01.004